

Strengthening the link between fullerenes and a subset of diffuse interstellar bands

Daniel Majaess^{1,2}  Tina A. Harriott^{1,2}  Halis Seuret,^{1,3} Cercis Morera-Boado^{1,4}  Lou Massa⁵ and Chérif F. Matta^{1,6,7,8} 

¹Department of Chemistry and Physics, Mount Saint Vincent University, Halifax, Nova Scotia B3M2J6, Canada

²Department of Mathematics and Statistics, Mount Saint Vincent University, Halifax, Nova Scotia, B3M2J6, Canada

³Centro de Investigaciones Químicas, IICBA, Universidad Autónoma del Estado de Morelos, Cuernavaca, 62209 Morelos, Mexico

⁴IXM–Cátedra Conacyt–Centro de Investigaciones Químicas, IICBA, Universidad Autónoma del Estado de Morelos, Cuernavaca, 62209 Morelos, Mexico

⁵Hunter College & the PhD Program of the Graduate Center, City University of New York, New York 10065, USA

⁶Department of Chemistry, Saint Mary's University, Halifax, Nova Scotia B3H3C3, Canada

⁷Département de Chimie, Université Laval, Québec G1V0A6, Canada

⁸Department of Chemistry, Dalhousie University, Halifax, Nova Scotia B3H4J3, Canada

Accepted 2025 March 11. Received 2025 March 11; in original form 2024 December 5

ABSTRACT

A debate persists regarding the correlation between the diffuse interstellar bands (DIBs) 9577 and 9632 Å, and whether they share a common molecular carrier (i.e. C_{60}^+). A robust high correlation determination emerges after bridging the baseline across an order of magnitude ($\simeq 50 - 700$ mÅ, $r = 0.93 \pm 0.02$), and nearly doubling the important higher equivalent width domain by adding new Mg II-corrected sightlines. Moreover, additional evidence is presented of possible DIB linkages to fullerenes, whereby attention is drawn to DIBs at 7470.38, 7558.44, and 7581.47 Å, which match the Campbell experimental results for C_{70}^+ within 1 Å, and the same is true of 6926.48 and 7030.26 Å for C_{70}^{2+} . Yet their current correlation uncertainties are unsatisfactory and exacerbated by expectedly low equivalent widths (e.g. $\overline{EW} = 4$ mÅ for 6926.48 Å), and thus further observations are required to assess whether they represent a *bona fide* connection or numerical coincidence.

Key words: Interstellar medium (ISM), nebulae – ISM: molecules.

1 INTRODUCTION

Galazutdinov et al. (2017, 2021), Schlarbmann et al. (2021), and Nie, Xiang & Li (2022) debated the correlation between the 9577 and 9632 Å diffuse interstellar bands (DIBs), which experiments highlight as prominent absorption features associated with C_{60}^+ (e.g. Fulara, Jakobi & Maier 1993; Campbell et al. 2015). Galazutdinov et al. (2021) argued those DIBs exhibit too low a correlation to be associated, or an unknown causes the correlation to vary (e.g. blended lines). Conversely, Schlarbmann et al. (2021) and Nie et al. (2022) favoured a high correlation and unambiguous link to C_{60}^+ . DIBs tied to 9365.2 and 9427.8 Å may also be associated with C_{60}^+ (Walker et al. 2016; Campbell, Holz & Maier 2016b; Lallement et al. 2018; Cordiner et al. 2019), although here too the conclusion is contested (Galazutdinov et al. 2021).

The topic is pertinent since C_{60}^+ is hitherto the sole carrier of DIBs where a consensus is coalescing (e.g. Cordiner et al. 2019; Nie et al. 2022). Several hundred other DIBs remain unassociated with specific molecules. Majaess et al. (submitted) advocated that the signatures of C–H, C=O, C≡C, C≡N, S–H, and aromatics (=C–H stretch, out-of-plane C–H bending, in-ring C=C, overtones) are discernible in energy differences between correlated DIBs in the Apache Point

Observatory catalogue (APO, Fan et al. 2019). Indeed, PAHs are hypothesized to be leading candidates for DIB sources (e.g. Bondar 2020; Weber et al. 2022), and efforts are likewise ongoing to explore the viability of fullerenes beyond C_{60}^+ (Section 2.2), heterofullerenes, and their (endo/exo)hedral inclusions (e.g. Omont 2016; Campbell et al. 2016a). A subset of those molecules may likewise explain the unidentified infrared emission lines (Sadjadi et al. 2020, 2022), in addition to MAONs (mixed aromatic/aliphatic organic nanoparticles; Kwok 2022; Kwok & Sadjadi 2023).

In this study, concerns regarding the correlation between the 9577 and 9632 Å DIBs are assuaged. Furthermore, additional DIBs are inspected whose source may also be connected to fullerenes (i.e. C_{70}^+ and C_{70}^{2+}), given tightly constrained matching wavelengths *vis à vis* laboratory results (Campbell et al. 2016a; Campbell, Holz & Maier 2017).

2 ANALYSIS

2.1 C_{60}^+ : 9577 and 9632 Å

Galazutdinov et al. (2021) concluded that the correlation between 9577 and 9632 Å is $r = 0.37$, whereas Schlarbmann et al. (2021) favoured estimates spanning 0.82–0.93. Nie et al. (2022) inspected

* E-mail: daniel.majaess@msvu.ca

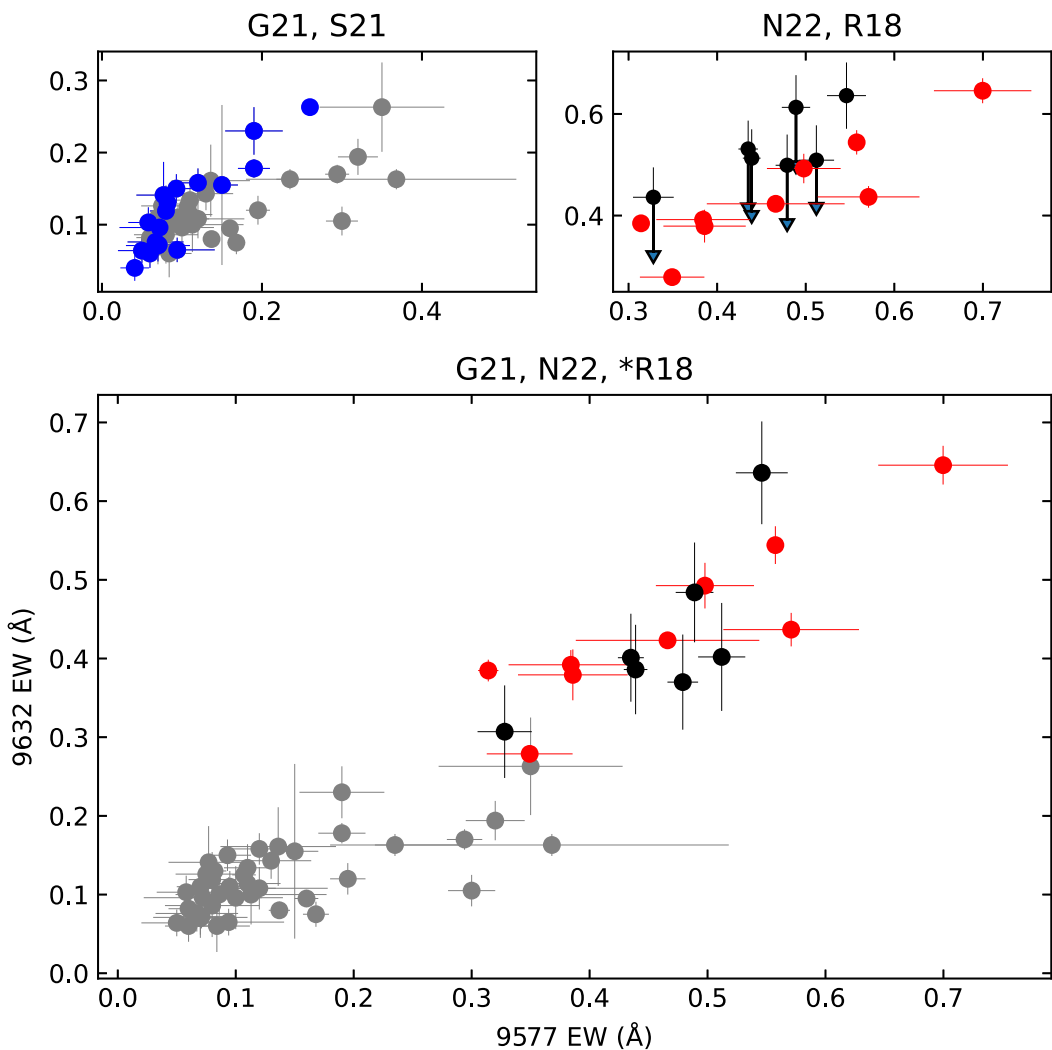


Figure 1. DIBs 9577 and 9632 Å are characterized by a high correlation across a sizable $\simeq 650$ mÅ EW baseline ($r = 0.93 \pm 0.02$; G21; N22; *R18). References correspond to Galazutdinov et al. (2021, grey), Schlarbmann et al. (2021, blue), and Nie et al. (2022, red). Advantageous higher EW sightlines were added from Ramírez-Tannus et al. (2018, black) since they mostly do not overlap with Nie et al. (2022), and were adjusted here for stellar Mg II contamination (bottom panel; *R18; see the text). Arrows in the top right panel convey the Mg II corrections. Table 1 highlights the dependence of r and the slope on permutations of the underlying data.

separate stars featuring higher equivalent widths (EWs) and advocated that $r = 0.89\text{--}0.96$.

It is argued here that the ambiguity partly arises from not bridging the analysis over a sizable EW baseline, whereby Galazutdinov et al. (2021) and Schlarbmann et al. (2021) sample relatively low EWs, Nie et al. (2022) data reside within a higher EW domain, and linking the data sets reveals a robust high correlation between 9577 and 9632 Å (Fig. 1, Table 1). Schlarbmann et al. (2021, their table 1) relied principally on Galazutdinov et al. (2021) data (Fig. 1, top left panel), and consequently the former is omitted from the final correlation determination (bottom panel of Fig. 1, $r = 0.93 \pm 0.02$).

Permutations of the data sets in concert with their slope and correlation determinations are conveyed in Table 1, which stemmed from an unweighted evaluation since the uncertainties are inhomogeneous. A firm high correlation remains in the absence of the Schlarbmann et al. (2021) data, or the adjusted Ramírez-Tannus et al. (2018) findings (Table 2). Regarding the latter, seven pertinent high EW data points were added from Ramírez-Tannus et al. (2018) once their uncorrected 9632 Å EWs were adjusted for stellar Mg II contamination. Those stars largely differ from the subsample presented by Nie

Table 1. Correlation and slope for 9577–9632 Å.

Data sets	$r \pm \Delta r$	$m \pm \Delta m$
G21, N22	0.92 ± 0.02	0.80 ± 0.04
S21, N22	0.98 ± 0.01	0.82 ± 0.05
G21, *R18	0.89 ± 0.03	0.77 ± 0.06
S21, *R18	0.96 ± 0.02	0.86 ± 0.05
G21, N22, *R18	0.93 ± 0.02	0.83 ± 0.04
S21, N22, *R18	0.97 ± 0.01	0.86 ± 0.04
G21, S21, N22, *R18	0.94 ± 0.01	0.83 ± 0.04

Note. References are Galazutdinov et al. (2021, G21), Schlarbmann et al. (2021, S21), and Nie et al. (2022, N22). Sightlines linked to comparatively cooler stars were added once corrected for stellar Mg II contamination (Ramírez-Tannus et al. 2018, *R18) (see the text).

et al. (2022) (B215 overlaps), who focused on hotter stars to mitigate the impact of Mg II. Tables 1 and 2 in Galazutdinov et al. (2017) include corrections for stars spanning diverse parameters (e.g. T_{eff} , metallicity, v_T , $\log g$), and a sigmoid was applied to approximate an upper bound Mg II– T_{eff} relation over the baseline examined:

Table 2. Ramírez-Tannus et al. (2018) original and corrected 9632 Å EWs.

CDS-Simbad ID	SpT	EW ₀ (mÅ)	EW _c (mÅ)
Cl* NGC6618 B215	B0-B1V	636±42	636±65
Cl* NGC6618 B243	B8V	499±34	370±60
Cl* NGC6618 B253	B3-B5III	509±47	402±69
Cl* NGC6618 B268	B9-A0	531±25	401±56
Cl* NGC6618 B275	B7III	513±27	386±57
Cl* NGC6618 B331	late-B	436±31	307±59
Cl* NGC6618 B337	late-B	613±39	484±63

Note. IDs and spectral types stem from Ramírez-Tannus et al. (2018). Their 9632 Å EWs were corrected (EW_c) for stellar Mg II contamination (see the text). A high correlation between 9632 and 9577 Å persists in the absence of the aforementioned data (Table 1).

Table 3. Candidate fullerene DIBs.

DIB (Å)	λ_e (Å)	Ion	λ_e (ref.)
7470.38	7470.2	C ₇₀ ⁺	Campbell et al. 2016a
7558.44	7558.4	C ₇₀ ⁺	Campbell et al. 2016a
7581.47	7582.3	C ₇₀ ⁺	Campbell et al. 2016a
6926.48	6927	C ₇₀ ²⁺	Campbell et al. 2017
7030.26	7030	C ₇₀ ²⁺	Campbell et al. 2017

Note. DIB wavelengths stem from the APO catalogue (Fan et al. 2019), save 7558.44 Å (Jenniskens & Desert 1994; Hobbs et al. 2009, see the text). λ_e are experimental wavelengths (Campbell et al. 2016a, 2017).

$\Delta EW \approx (130 \pm 50 \text{ mÅ})(1 - (1 + e^{(20200 - T_{\text{eff}})/1751})^{-1})$. Corrections emerging from that approximation were subsequently applied to the seven stars using spectral types from Ramírez-Tannus et al. (2017, 2018),¹ and their corresponding temperatures stemmed from unpublished data by D. G. Turner (e.g. used in Turner 1994, and references therein). Uncertainties for the corrected 9632 Å Ramírez-Tannus et al. (2018) EWs were all expanded in quadrature by a bulk 50 mÅ from their original values. Table 2 underscores that the corrections shift the original Ramírez-Tannus et al. (2018) data downwards in Fig. 1 (top right panel) and upon the Nie et al. (2022) observations. Otherwise, the initial Ramírez-Tannus et al. (2018) EWs are too high, and discernibly offset from the Nie et al. (2022) data. As noted Nie et al. (2022) do not require corrections owing to their hotter temperature sample. That in sum reaffirms that the approximated Mg II corrections are satisfactory for the present purpose, despite the uncertainties (e.g. deviations from the mean trend, SpT, T_{eff} , possible Doppler offsets between Mg II and the DIB, and for the latter see fig. 4 in Galazutdinov et al. 2017). Lallement et al. (2018) and Galazutdinov et al. (2021) debated the Mg II corrections employed by Galazutdinov et al. (2017), and for additional approaches to the problem consider Jenniskens et al. (1997) and Walker et al. (2016). A comprehensive spectral analysis comparing differing atmospheric models is desirable but beyond the scope of this current effort, especially given the scaffolding underpinning Table 1 and the consistently high correlation conclusion.

2.2 The C₇₀⁺ and C₇₀²⁺ DIB families

There may be DIBs tied to other fullerenes (e.g. C₇₀⁺, C₇₀²⁺, Table 3). Those lines could help demarcate mid-infrared vibrations, whereby energy differences among DIBs within the family (e.g. highly

¹A B8 temperature class was assumed when Ramírez-Tannus et al. (2018) relayed a ‘late-B’ classification.

Table 4. DIB correlations, slopes, and lab attenuation ratios.

DIB (Å)	\overline{EW} (mÅ)	DIB (Å)	n	r	m	R_a
				$\pm \Delta r$	$\pm \Delta m$	$\pm \Delta R_a$
C ₇₀ ⁺	7470.38	7557.88	12	0.84	2.6	1.0
				± 0.10	± 0.5	± 0.3
				0.80	4.2	1.3
C ₇₀ ²⁺	6926.48	7581.47	14	± 0.10	± 0.8	± 0.4
				0.76	1.6	1.3
				± 0.13	± 0.4	± 0.4
	7557.88	7581.47	9	0.84	0.8	2.0
				± 0.12	± 0.2	± 0.6

Note. DIB wavelengths and EWs from the APO catalogue (Fan et al. 2019). Low statistics and EWs, and a limited baseline, suggest the uncertainty is larger than cited.

correlated EWs) could represent separate vibrational modes. Experimental wavelengths for C₇₀⁺ and C₇₀²⁺ were adopted from Campbell et al. (2016a, 2017), and compared to published DIB wavelengths (Jenniskens & Desert 1994; Hobbs et al. 2009; Bondar 2012; Fan et al. 2019). For C₇₀⁺ the following DIBs align with experimental results to within 1 Å: 7470.38, 7558.44, and 7581.47 Å. Campbell et al. (2016a) relay that the most prominent laboratory C₇₀⁺ line (7632.6 Å) shall be severely contaminated by telluric absorption, and hence the motivation for satellite measurements (e.g. Cordiner et al. 2019). Furthermore, APO catalogue DIBs linked to 6926.48 and 7030.26 Å may be indicative of C₇₀²⁺, again owing to their wavelength proximity relative to experimental determinations (Campbell et al. 2017). Regarding the Campbell et al. (2016a) laboratory C₇₀⁺ wavelength at $\lambda_e = 7558.4$ Å, Jenniskens & Desert (1994) and Bondar (2012) feature DIBs at 7558.5 and 7559.19 Å, respectively. That is supported by Hobbs et al. (2009), who characterized DIBs at 7558.44 and 7559.48 Å, with the former being numerically coincident with the experimental result of 7558.4 Å (Table 3). The Fan et al. (2019) compilation possesses lines bracketing the laboratory measurement at 7557.88 and 7559.43 Å, which in tandem with the aforementioned Hobbs et al. (2009) DIBs, could represent the same vibrational line with differing rotation.²

An effort was undertaken to (in)validate the wavelength analysis by one tied to correlations (Table 4). EWs and wavelengths were adopted from Fan et al. (2019) given their sample size (i.e. number of sightlines $n \geq 9$). Unweighted correlations that emerged include $r = 0.84 \pm 0.10$ for the 7470.38–7557.88 Å DIB pair (Table 4), and $r = 0.80 \pm 0.10$ for 7470.38–7581.47 Å (Fig. 2). The correlation evaluations are merely suggestive owing partly to the impact on uncertainties from expectedly³ low EWs (e.g. 7470.38 Å has a median $\overline{EW} = 5$ mÅ). That uncertainty likewise complicates a comparison between low interstellar EWs and relative laboratory attenuation (R_a , Table 4), which measure separate marginal (in this instance) quantities in differing environments. For example, experiments implied that $\lambda_e = 7470.2$ Å exhibits a lower intensity than 7582.3 Å (Campbell et al. 2016a), and that is apparent in Fig. 2. The slope characterizing those DIB EWs ($m = 4.2 \pm 0.8$) is larger than an indirect comparison to the relative lab-measured attenuation ($R_a \sim 1.3$). As noted above, it is also unclear whether the highly correlated APO catalogue lines of 7557.88 and 7559.43

²That may likewise be true of the Fan et al. (2019) 5779.59 and 5780.64 Å DIBs (Smith et al. 2021).

³Campbell et al. (2016a, 2017).

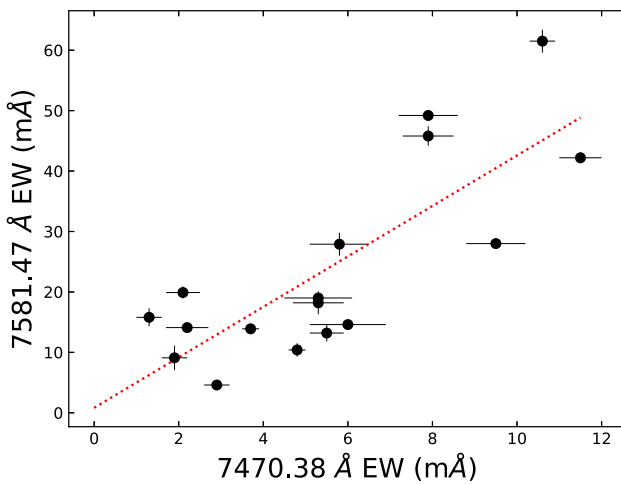


Figure 2. Correlation analysis between two DIBs (7470.38–7581.47 Å) which exhibit wavelengths comparable to experimental C_{70}^+ lines (Table 3). The expected low EWs ($\lambda_e = 7470.38 \text{ \AA}$, Campbell et al. 2016a) help expand the correlation uncertainty ($r = 0.80 \pm 0.10$). The slope ($m = 4.2 \pm 0.8$) is larger than an indirect comparison to the relative lab-measured attenuation (R_a , Table 4).

Å ($r = 0.92 \pm 0.05$, $n = 16$) constitute a single vibrational line, and the EWs must be combined prior to a comparison with experimental results. Additional observations across a sizable EW baseline may clarify whether the DIBs belong to fullerene carriers, or represent a numerical coincidence. Yet reliably measuring such low EWs poses a challenge, especially given the experimental full width at half-maximum (FWHM), as noted previously (Campbell et al. 2016a, 2017).

3 CONCLUSIONS

DIBs linked to the buckminsterfullerene cation at 9577 and 9632 Å are highly correlated (Fig. 1, $r = 0.93 \pm 0.02$). That assessment stemmed from an analysis spanning a lucrative EW baseline, and bridging low to high EWs provides a confident conclusion. The EWs were tied to existing (Galazutdinov et al. 2021; Nie et al. 2022) and newly corrected estimates (Ramírez-Tannus et al. 2018). Regarding the latter, 9632 Å data points linked to relatively cooler stars within Ramírez-Tannus et al. (2018) were corrected here for Mg II contamination (top right panel of Fig. 1). Their addition reaffirms the overarching conclusion of a high Pearson correlation (Table 1).

The analysis was expanded to identify DIBs associated with fullerenes beyond C_{60}^+ (i.e. C_{70}^+ and C_{70}^{2+}). Several DIBs overlap with the Campbell et al. (2016a, 2017) laboratory wavelengths to within an Angstrom (Table 3; e.g. DIB 7558.44 Å and $C_{70}^+ \lambda_e = 7558.4 \text{ \AA}$). A complimentary correlation analysis was limited by low EWs and statistics (Fig. 2, Table 4, e.g. $\overline{EW} = 4 \text{ m\AA}$ for 6926.48 Å). Additional observations over an extensive EW baseline are required to assess whether those DIBs are linked to fullerene cations. The

current evidence, though inconclusive, provides sufficient impetus to pursue such observations. Future work may include relinquishing a strict $< 1 \text{ \AA}$ criterion, and exploring matches relative to fractionary offsets within an FWHM (e.g. $|\text{DIB} - \lambda_e| < \frac{1}{x} \text{ FWHM}$).

ACKNOWLEDGEMENTS

This research relied on initiatives such as Campbell et al., APO Catalog of DIBs, CDS, NASA ADS, arXiv.

DATA AVAILABILITY

The data underlying this article are available via the Centre de Données astronomiques de Strasbourg (CDS), and references such as Fan et al. (2019) and Campbell et al. (2016a, 2017).

REFERENCES

- Bondar A., 2012, *MNRAS*, 423, 725
- Bondar A., 2020, *MNRAS*, 496, 2231
- Campbell E. K., Holz M., Gerlich D., Maier J. P., 2015, *Nature*, 523, 322
- Campbell E. K., Holz M., Maier J. P., Gerlich D., Walker G. A. H., Bohlender D., 2016a, *ApJ*, 822, 17
- Campbell E. K., Holz M., Maier J. P., 2016b, *ApJ*, 826, L4
- Campbell E. K., Holz M., Maier J. P., 2017, *ApJ*, 835, 221
- Cordiner M. A. et al., 2019, *ApJ*, 875, L28
- Fan H. et al., 2019, *ApJ*, 878, 151
- Fulara J., Jakobi M., Maier J. P., 1993, *Chem. Phys. Lett.*, 211, 227
- Galazutdinov G. A., Shimansky V. V., Bondar A., Valyavin G., Krełowski J., 2017, *MNRAS*, 465, 3956
- Galazutdinov G. A., Valyavin G., Ikhsanov N. R., Krełowski J., 2021, *AJ*, 161, 127
- Hobbs L. M. et al., 2009, *ApJ*, 705, 32
- Jenniskens P., Desert F. X., 1994, *A&AS*, 106, 39
- Jenniskens P., Mulas G., Porceddu I., Benvenuti P., 1997, *A&A*, 327, 337
- Kwok S., 2022, *Ap&SS*, 367, 16
- Kwok S., Sadjadi S., 2023, in AAS Meeting Abstracts. p. 144.07
- Lallement R. et al., 2018, *A&A*, 614, A28
- Nie T. P., Xiang F. Y., Li A., 2022, *MNRAS*, 509, 4908
- Omont A., 2016, *A&A*, 590, A52
- Ramírez-Tannus M. C. et al., 2017, *A&A*, 604, A78
- Ramírez-Tannus M. C., Cox N. L. J., Kaper L., de Koter A., 2018, *A&A*, 620, A52
- Sadjadi S., Kwok S., Cataldo F., García-Hernández D. A., Manchado A., 2020, *Fuller. Nanotub. Car. N.*, 28, 637
- Sadjadi S., Parker Q. A., Hsia C.-H., Zhang Y., 2022, *ApJ*, 934, 75
- Schlarmann L., Foing B., Cami J., Fan H., 2021, *A&A*, 656, L17
- Smith F. M., Harriott T. A., Majaess D., Massa L., Matta C. F., 2021, *MNRAS*, 507, 5236
- Turner D. G., 1994, *JRASC*, 88, 176
- Walker G. A. H., Campbell E. K., Maier J. P., Bohlender D., Malo L., 2016, *ApJ*, 831, 130
- Weber I., Tsuge M., Sundararajan P., Baba M., Sakurai H., Lee Y.-P., 2022, *J. Phys. Chem. A*, 126, 5283

This paper has been typeset from a TeX/LaTeX file prepared by the author.